ISSN 1672-9145 Acta Biochimica et Biophysica Sinica 2004, **36**(12): 803–810 **CN** 31-1940/Q

Correlation of Behavior Changes and BOLD Signal in Alzheimer-like Rat Model

Zheng-Hui HU[#], Xiao-Chuan WANG[1#], Li-Yun LI[3], Mai-Li LIU[3], Rong LIU[1], Zhiqun LING[1], Qing TIAN[1], Xiao-Wei TANG, Yi-Gen WU[2]*, and Jian-Zhi WANG[1]*

Department of Physics and Bio-X disciplinary Laboratory, Zhejiang University, Hangzhou 310027,China;
[1]Department of Pathophysiology, Tongji Medical College, Huazhong University of Science and Technology, Wuhan 430030, China;
[2]Institute of High Energy Physics and Key Laboratory of Nuclear Analysis Techniques, Chinese Academy of Sciences, P.O. Box 918, Beijing 100039, China;
[3]Wuhan Institute of Physics and Mathematics, State Key Laboratory of Magnetic Resonance and Atomic and Molecular Physics, Chinese Academy of Sciences, Wuhan 430071, China

Abstract To explore a potential means for the early diagnosis of Alzheimer disease, we studied the relationship of resting T2* signal and tau hyperphosphorylation/spatial memory deficit. The rat model with tau hyperphosphorylation and spatial memory deficit was established by bilateral hippocampi injection of isoproterenol (IP). Then, the correlative alteration between resting T2* signal and spatial memory retention was assessed with blood oxygenation level dependent (BOLD) functional magnetic resonance imaging (fMRI) study and Morris Water Maze test, and Western blot was employed to confirm tau hyperphosphorylation. The analysis showed following results. (1) Tau phosphorylation at Ser^{396}/Ser^{404} and Ser^{199}/Ser^{202} was significantly increased in IP-injected rats as detected by PHF-1 and tau-1, respectively. (2) An AD-like spatial memory retention disturbance was induced at 24 h after isoproterenol injection. (3) A sensitivity threshold of resting T2* signal intensity, which separated the IP-treated rats from vehicle control, was obtained by applying linear regression analysis, and an estimated sensitivity statistical threshold was at 32.62. These results suggest that resting T2* signal may serve as a noninvasive quantitative marker in predicting AD-like spatial memory deficits and tau hyperphosphorylation.

Key words Alzheimer disease (AD); functional magnetic resonance imaging (fMRI); isoproterenol (IP); Morris Water Maze; diagnosis

Memory impairment is usually the early and most prominent clinical manifestation of Alzheimer disease (AD), a progressive neurodegenerative illness characterized by gradual deposition of neuritic plaques and neurofibrillary tangles in the brain of the patients [1–3]. Knowledge of life expectancy after the diagnosis of AD and characteristics of cured patients may help future therapy [4,5].

Received: August 25, 2004 Accepted: October 25, 2004
This work was supported by the grants from the Natural Science Foundation of China (No. 39925012, No. 30100057, and No. 30170221), the Major State Basic Research Development Program of China (G1999054007, G19990504006) and National Educational Committee of China (2001-171)
[#]These authors contributed equally to this work
*Corresponding authors:
Jian-Zhi WANG: Tel, 86-27-83692625; Fax, 86-27-83693883; E-mail, wangjz@mails.tjmu.edu.cn
Yi-Gen WU: Tel, 86-10-88233185; Fax, 86-10-88233186; E-mail, wuyg@ihep.ac.cn

Increasing efforts have been made these years in establishing noninvasive means to diagnose AD. Much attention is paid on the hippocampus region, which is a part of the mesial temporal lobe memory system and is affected in the early stage of AD pathology [6]. Hippocampus atrophy, measured with high-spatial-resolution magnetic resonance (MR) imaging of the brain, has shown important diagnostic value [7,8]. The cross-correlation coefficients of spontaneous low frequency (COSLOF) index measured in the human hippocampus has been proposed as a noninvasive marker of probable AD patients [9]. Nevertheless, these methods are questionable due to the lack of sensitivity and specificity [10], and there is still no definite clinical diagnosis means for AD up to now.

Functional imaging of brain with magnetic resonance imaging (MRI) becomes popular in neuroscience, but conventional task-driven paradigms are mainly limited on

studying brain diseases in which it is difficult to obtain patients participation considering impaired cognition ability. Recently, a novel, non-task-related magnetic resonance imaging approach that relied on a resting rather than dynamic signal was developed [11]. This method provides indirect measurement of the changes in resting neuronal metabolism occurs with relatively subtle changes in brain function. Its application led to the discovery that hippocampus signal was significantly diminished in elderly subjects with memory decline compared to age-matched control, and different subjects showed dysfunction in different subregion [11]. By this means, we also reported a negative correlation between tau hyperphosphorylation and BOLD signal intensity in hippocampus and cortex area of isoproterenol-injected rats [12].

In the present study, we further investigated the correlation between the resting T2* signal and memory retention deficits by using the isoproterenol-treated rats.

Material and Methods

Drugs and reagents

Isoproterenol (IP, Sigma, St. Louis, MO, USA) was diluted in normal saline (NS) with a final concentration of 20 mM for instant application [13]. Anti-tau antibodies are listed in Table 1. Histostain-SP detection kit for immunohistochemistry was from Zymed (South San Francisco, CA, USA).

Rat brain infusion

Male Wistar rats (2 months old, 275 g, Grade II, Certificate No. TJLA2000-3) were from Faculty of Laboratory Animal (Tongji Medical College of HUST, China), and maintained according to "Chinese Regulations for Experimental Animals" for 9 days. Rats were anaesthetized with 6% chloral hydrate (*W*/*W*; 6 ml/kg, i.p.), and then placed on a stereotaxic apparatus. The skull was exposed by an incision in scalp and the position of the rat was adjusted so that the bregma and lambda were in the same horizontal plane. Bilateral holes were drilled with a 1.8-mm trephine above the hippocampus region using the following coordinates, 4.8 mm anterior to posterior (AP) bregma, 2.2 mm midline to lateral (ML). With a 5-μl microsyringe, bilateral injections of 2 μl 20 mM isoproterenol were made 3.0 mm dorsal to ventral (DV) dura [14]. The needle was remained in place 5 min to allow diffusion of solution [13]. Same volume of NS was injected as vehicle control. The scalp incision was immediately sutured. Rats were allowed to recover for 2 days with free access to water and food.

Morris Water Maze test

The water maze was a circular tank made of stainless steel with 2 m in diameter and 0.6 m in height. It was positioned in the middle of a dimly light (30 lx) testing room enriched with distal visual stimuli. The bottom of the maze was raised 0.35 m above the floor. At the beginning of each day, the tank was filled with a tap water to a depth of 0.3 m, and the water temperature was maintained at (26 ± 2) °C. Four points, equally spaced along the circumference of the pool, were arbitrarily designated as N, E, S, and W. The area of the pool was also conceptually divided into four quadrants (NE, SE, SW and NW) of equal size by two imaginary diagonal lines running through the center of the pool. A stable circular platform, measuring 10 cm in diameter and wrapped with white cloth, was submerged 2 cm below the surface of the water made opaque with milk powder to escape the platform from the rat's view. The rim of the pool is 1.0 m from the nearest visual cue of red and blue marks. A video camera, connected to an image analysis system, which in turn was connected to a microcomputer running the software, was mounted above the center of the water maze. The swimming path of the animal was tracked, digitized and stored for subsequent behavioral analysis using the same software. Each trial was started and ended manually by the experimenter. Both latency times and swimming distances before reaching the platform were measured.

The rat was brought to the sight and acclimatized for

Table 1 Tau antibodies employed in this study

Antibody	Type	Specificity [a]	Phosphorylation sites [b]	Dilution
R111e	Polyclonal	unP+P	–	1:5000
tau-1	Monoclonal	unP	Ser^{199}/Ser^{202}	1:30,000
PHF-1	Monoclonal	P	Ser^{396}/Ser^{404}	1:500

P, phosphorylated epitope; [a] unP, unphosphorylated epitope; [b] numbered according to the largest isoform of human brain tau.

two hours, and then lowered gently into the water, with its head facing the wall of the water maze. The trial ended when the rat climbed onto the platform. Before each trial, the rat was given a maximum of 60 s to find the hidden platform and was allowed to remain on it for 30 s. Rats that failed to locate the platform within 60 s were guided to the platform by the experimenter. Each training session consisted of 4 trials altogether (one trial per quadrant) with 30 s interval, and the training lasts for seven days [15]. On the eighth day rats were trained as usual and their escape latency and swimming path were recorded as primary protocols.

The rats were returned to the water maze 24 h after isoproterenol or saline injection for memory retention test.

Western blots

The phosphorylation of tau was analyzed by Western blot using 10% SDS-PAGE as described originally by Laemmli. The separated proteins were transferred on Immobilon-P membrane (Millipore, Bedford, MA, USA) and probed with phosphorylation dependent tau antibodies, tau-1 (recognize unphosphorylated tau at Ser^{199}/Ser^{202}), PHF-1 (recognize phosphorylated tau at Ser^{396}/Ser^{404}) and polyclonal antibody R111e (reacts with total tau), kind gifts from Dr. Binder (Northwestern University, Chicago, Illinois, USA), Dr. Davis (Albert Einstein College of Medicine, Bronx, NY, USA) and Dr. Iqbal (New York State Institute for Basic Research, Staten Island, NY, USA), respectively. The blots were developed with peroxidase-conjugated secondary antibody from Amersham Pharmacia Biotech (Little Chalfort, Buckinghamshire, England) and visualized with enhanced chemiluminescence (ECL) system.

BOLD fMRI studies

After the rat was anaesthetized with 6% chloral hydrate (*W*/*W*; 6 ml/kg, i.p.), it was placed prone in a cradle and its head was secured with a bite-bar and tightly fixed by foam cushions on both sides of the head to minimize head movement.

The fMRI data were obtained on a horizontal-bore 4.7T spectrometer (Bruker Biospec 47/30) in Wuhan Institute of Physics and Mathematics, Chinese Academy of Sciences. The center of the special radio-frequency surface-coil (10 mm diameter) was placed above the bregma and static magnetic field homogeneity was optimized on axial slices. A gradient echo imaging sequence (T2*-weighted, echo time 25 ms, repeat time 560 ms) was selected to maximize the blood oxygen level-dependent contrast. Interleave sampling was applied to avoid interference between adjacent layers. Each brain image volume was acquired in 14 slices, each being 1-mm thick with 0.2-mm gap between adjacent layers and comprising 256×256 pixels (in-plane spatial resolution was 0.234 mm×0.234 mm). Each scanning session consist of about 35 image volumes. Acquisition time of each image volume was 1 min and 11 s. IP- and NS-treated rats were imaged in a random order, and operation type was not known to the investigator. All data were acquired under steady-state conditions without inflicting any stimulus.

Image processing and data analysis

Image processing and statistical analysis were performed using SPM99 (Welcome Department of Cognitive Neurology, London, UK; http://www.fil.ion.ucl.ac.uk). Firstly, to correct dislocations caused by head motion, all resting T2* images were realigned. Then, these images were transformed into 'standard brain space' using the parameter obtained from the normalization process of the functional image that was coregistered to the first image beforehand. In our study, the space of the template images used in statistical parametric mapping (SPM) for image normalization is based on NS-treated group. The stereotactic space is derived from 8 NS-treated rat brains. Finally, for smoothing, a 3D convolution was applied to the images using a Gaussian kernel with a vector of length 3 (0.469 mm, 0.469 mm, 2 mm) for anisotropic voxels in the group analysis.

The preprocessed data were analyzed with statistical parametric mapping. The effect of global differences in scan intensity was removed by Ancova model [16], which supposed that the relationship between regional and global variation was approximately linear. Statistical analysis of resting T2* signal changes was performed by "General Linear Model" [17]. Since resting T2* signal based on nontask-related magnetic resonance imaging is not time series, a "multi-subject: covariates only" model which is ordinarily done in positron emission tomography (PET) is employed. This model can be extended by adding subject effects to give single subject activation model, which is a simple linear regression at voxel:

$$Y_j^k = \gamma_j^k + \zeta_j^k (g_{ij} - \bar{g}_{\bullet\bullet}) + \varepsilon_{ij}^k$$

where Y_j^k denotes response variable (signal intensity) at voxel k of scan j=1,…,M in subject i=1,…, N; $\bar{g}_{\bullet\bullet}$ denotes the mean of subject means; g_{ij}, denotes the global mean at scan j=1, …,M in subject i=1, …N; γ_j^k is the response variable after removing global effects; and ζ_j^k is the factor of global effects. The model assumed that the errors ε_{ij}^k are independent, vary with voxels, and are identically distri-

buted normal random variables with zero mean and variance σ^2. So ε_{ij}^{k} can be written in

$$\varepsilon_{ij}^{k} \overset{iid}{\sim} N(0,\sigma^2)$$

In this case the model is over-determined (i.e., design matrix is rank deficient), and has infinitely many parameter sets describing the same model. Correspondingly, there are infinitely many least squares estimates satisfying the normal equations. Here a sum-to-zero constraint on the fitted group effects

$$\sum_{q=1}^{Q} \hat{\alpha}_q = 0$$

where α_q denotes weight in condition q=1,⋯,Q, is imposed on the estimates. This constraint implies that any one group's fitted effect is minus the sum of the others, so the constraint can be effect by expressing the effect for the last group in terms of the others and eliminating it from the design. Therefore, an appropriate contrast with weights would be $c=(1/6,1/6,1/6,1/6,1/6,1/6,c_7,c_8,\cdots,c_{13})^T$ for single subject statistic assess in this study. For example, a contrast with weights of c^T=(1/6,1/6,1/6,1/6,1/6,1/6, –1,0,0,0,0,0,0) assesses the change of BOLD signal, subtracting the signal intensity in whole sham-operated group from that in the first IP-operated rat.

Finally, a correlated Student's *t*-test was applied to find out decreased signal intensity in individual IP-treated rat compared with vehicle group, and resulting brain images that were then transformed to a unit-normal distribution with a given threshold *T* (*T*>30, uncorrected). Any region that consisted of less than eight-clustered voxels was not considered to be a significant signal and was thus excluded.

Results

Induction of AD-like tau hyperphosphorylation by injection of isoproterenol

Studies have suggested that PKA is one of the key kinases participating tau hyperphosphorylation. Therefore, we used isoproterenol to activate PKA in rats, and the results were shown in Fig. 1. Western blot anaysis showed

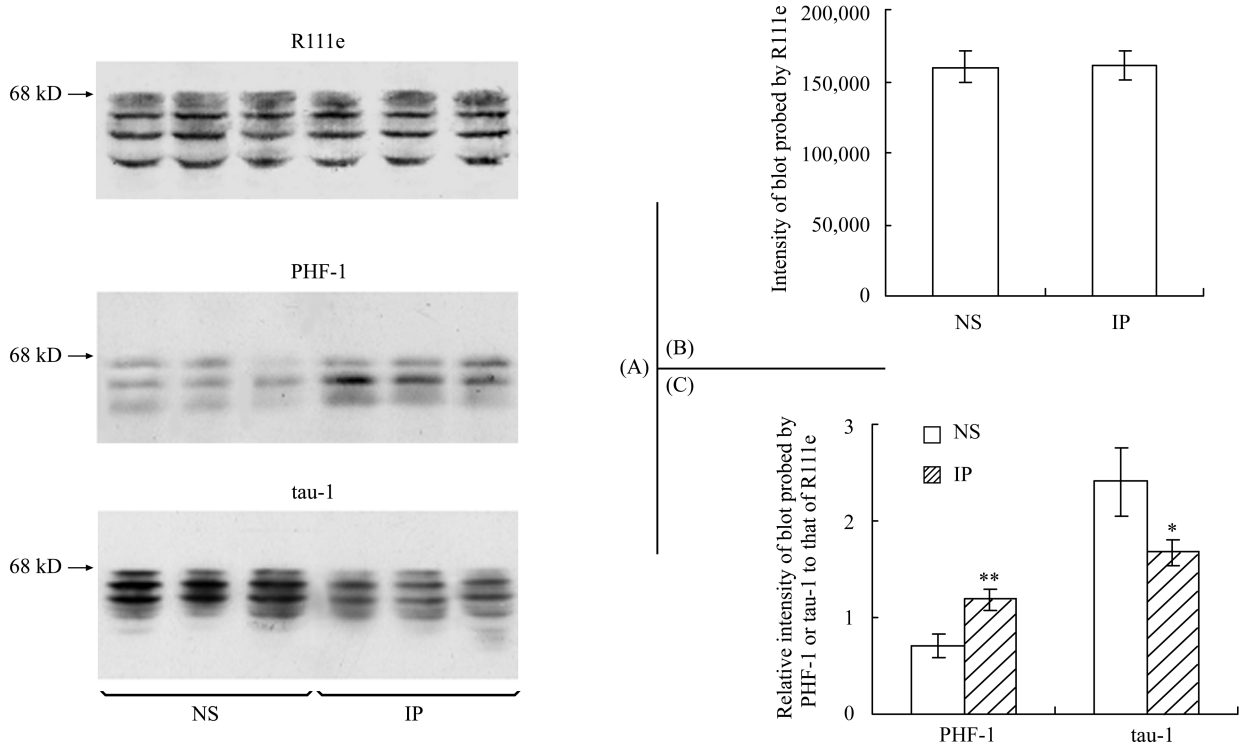

Fig. 1 Induction of tau hyperphosphorylation by isoproterenol

(A) Western blots of tau extracted from rat hippocampus after injection of IP or NS for 24 h. The blots were probed by R111e (15 μg protein per lane), PHF-1 (30 μg of protein per lane) or tau-1 (15 μg protein per lane) as indicated, respectively. Hyperphosphorylation of tau at both tau-1 and PHF-1 epitopes was observed. (B) Densitometric analysis of R111e. No significant alteration in total level of tau probed by R111e. (C) Relative density of tau probed by PHF-1 and tau-1 normalized against that probed by R111e. NS, normal saline; IP, isoproterenol. **P*<0.05 vs. NS group; ***P*<0.01 vs. NS group.

that the hyperphosphorylation of tau at both tau-1 and PHF-1 epitopes was induced by isoproterenol, demonstrated by significantly increased immunoreaction to PHF-1 and decreased staining to tau-1 in isoproterenol rats than vehicle control rats. The level of phosphorylated tau at above sites was normalized by total level of tau, which was not altered by IP (Fig. 1). These data suggest that isoproterenol induces tau hyperphosphorylation at Ser^{396}/Ser^{404} (PHF-1) and Ser^{199}/Ser^{202} (tau-1) sites.

Induction of memory retention deficits by injection of isoproterenol

Morris Water Maze was employed to investigate how spatial memory retention was altered in the isoproterenol-injected rats. After pre-training for a week, all rats can directly swim to the hidden platform within 10 s. Then these rats were randomly divided into two groups received injection of isoproterenol and saline, respectively. The memory retention test data at 24 h after infusion showed that the escape latency to find the hidden platform in IP-treated rats was remarkably prolonged in comparison with that of pre-surgery group [(49.83 ± 8.65) s vs. (6.55 ± 2.42) s, $P<0.01$, Fig. 2], while the escape latency of saline rats did not change significantly [(10.44 ± 5.78) s vs. (6.74 ± 2.37) s, $P=0.14$], and significant differences was also observed between the IP- and NS-treated group [(49.83 ± 8.65) s vs. (10.44 ± 5.78) s, $P<0.01$, Fig. 2]. The results of the swimming pathway showed that IP-injected rats swam randomly rather than directly to the hidden platform compared with the NS rats or the pre-surgery group (Fig. 3).

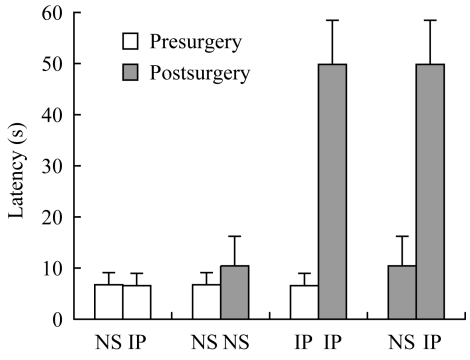

Fig. 2 Induction of memory retention deficits by injection of isoproterenol

The rats were trained for (7+1) days in Morris Water Maze pre-surgery as described in "Materials and Methods". The memory retention test showed an increased latency to find the hidden platform in IP-injected rats, while no significant difference was found between pre-surgery and post-surgery NS-rat. $^{**}P < 0.01$ vs. NS group.

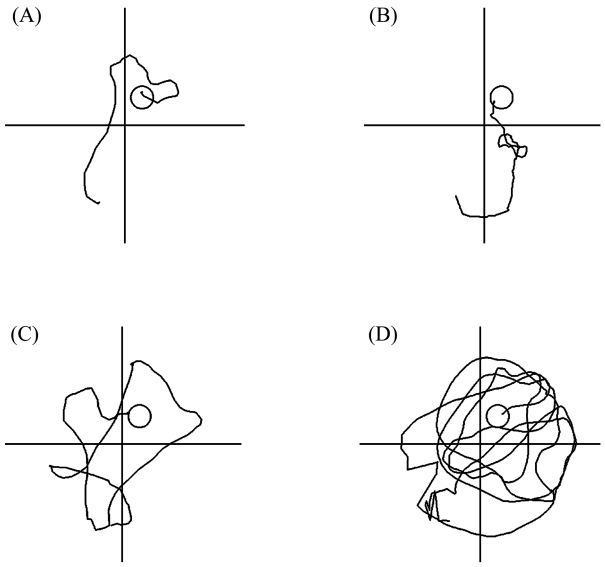

Fig. 3 Representative swimming pathway of rats taken from their starting position at Northeast to the hidden platform at Southwest in the water maze

(A,C) and (B,D) were from NS and IP group, respectively. (A,C) Indicated swimming pathway from the typical rat after a seven-day training pre-surgery. (B,D) Indicated swimming pathway of the same rat 24 h post-surgery. Note that the IP-injected rat lost its directional bearings and thus employed more random search strategy than straight search strategy. NS-treated rat did not change much in the pathway to find the hidden platform.

Alterations of resting T2* signal in IP-treated rats and the correlation with memory retention

The analysis of functional imaging experiments often involves the formation of a statistical parametric map. In such maps, the value at each voxel is a statistic that expresses evidence against a null hypothesis of no experimentally induced difference at that voxel. In order to decide, at a give level of significance, which parts of the brain were activated, the inference (threshold) method was applied. Ordinarily these involve in selecting a significance (P or T) threshold and applying this to every voxel in the statistic map. Nevertheless, the choice of the threshold is usually quite arbitrary, especially for generalized conclusion to different population. We attempted to fix it through relating neurophysiologic parameters with behavior changes of the rats. We first defined the region-of-interest (ROI) in hippocampus of rats (Fig. 4). The ROI used in the present study was 1.5 mm×6 mm×1.5 mm containing primarily hippocampus. For any given voxel of this region, an analysis of variance done separately at each voxel, whereafter t-test for each voxel was made from the results of this analysis to get an image of statistical analysis.

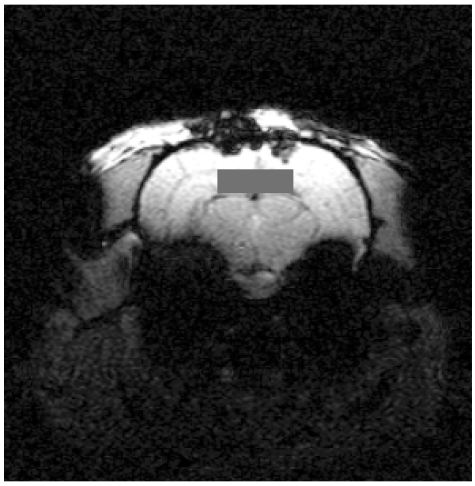

Fig. 4 The location of the region-of-interest containing primarily hippocampus

Black rectangle indicated the location of ROI. Magnification was 4×.

The maximal *T* value within this region that represented alteration of memory retention in IP-injected rats was selected for further analysis. As we predicted, the alteration of *T* value was positively correlated with increased escape latency in IP-treated rats (Fig. 5). The *L* values representing alterations in memory retention measured by water maze were ranged from 31.33 to 55.23 with a confidence level of 99%, whereas the minimum *T* value representing resting T2* signal received by BOLD fMRI should be larger than 30 to assure a better representative for probing sensitivity of this model.

Based on the estimation mentioned above, the threshold of the *t*-test index, which differentiates the validity of this model, can be set around 30. The difference between NS-rats were tested directly and IP-injected rats for every voxel in the brain to produce an SPM{*t*} showing voxels in which intensity of IP-injected rats decreased relative to NS-operated subject. A threshold of $T>30$ was used for the contrast.

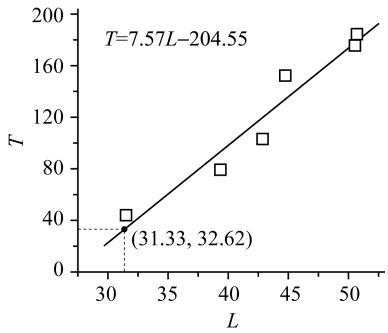

Fig. 5 Linear fit between sensitivity threshold *T* and escape latency *L* as a function of memory loss

Positive correlation, i.e., $T=7.57L-204.55$ was received, and the estimated minimum resting T2* signal sensitivity threshold was 32.62 with confidence level of 99%. *T*, sensitivity threshold; *L*, escape latency.

The correlation between resting T2* signal and escape latency was estimated by a simple regression analysis as

$$T=7.57L-204.55$$

where *T* is a statistical parameter that represents difference of T2* signal between individual IP-treated rat and mean value of NS rats, and *L* is the difference of escape latency in IP-treated rats between pre-surgery and post-surgery. By using this regression function, correlation between any given minimum value of difference detected by Morris Water Maze and *T* value for the validation of fMRI that may serve as a differential sensitivity threshold for credibility of animal models can be estimated.

Discussion

Until now, a confirmative diagnosis of AD is still exclusively relying on the appearance of numerous senile plaques and neurofibrillary tangles detected during postmortem brain autopsy. It is reported that the severity of dementia is positively correlated to the amount of neurofibrillary tangles in brain of AD patients [18], which is composed of bundles of paired helical filament of abnormally hyperphosphorylated tau [19]. Accumulating data suggest that phosphorylated tau (p-tau) may serve as a biochemical marker in the diagnosis of AD. For example, p-tau phosphorylated at threonine 181 (Thr^{181}) improved diagnostic accuracy between AD and dementia with Lewy bodies; p-tau phosphorylated at serine 199 (Ser^{199}) demonstrated high discriminative power between AD and non-AD dementia; p-tau phosphorylated at Ser^{396}/Ser^{404} improved differential diagnosis between AD and vascular dementia [20,21]. Based on this knowledge, we established an AD-like tau hyperphosphorylation model by hippocampi infusion of isoproterenol, a PKA activator. Tau hyperphosphorylation in model rats was confirmed by immunocytochemistry previously [12], and quantitatively analyzed by Western blot in the present study. And positive correlation of tau hyperphosphorylation and spatial memory retention deficits was observed in isoproterenol injected model rats.

As a neural protein, tau can only be detected in cerebrospinal fluid (CSF), so measuring total tau or p-tau [20,

22] is very limited because of the restriction in obtaining CSF samples. This brings forward the challenge and urgency to search for non-invasive means. Previous findings suggest that BOLD activation may actually reflect the neural activity related to the input and the local processing in any given area [23]. Neurodegenerative progression can induce a decrease in the activity of the cells that are projecting to the related areas, which can be reflected on the change of T2* signal. The sensitivity and spatial resolution of resting T2* imaging make it be an ideal modality for assessing these relatively subtle changes in brain. The present study attempted to relate neurophysiologic parameters with behavior changes of the rats. Then, a linear regression analysis applied to fMRI data provided a potential approach as minimum sensitivity threshold for behavior changes in an AD-like rat model. Furthermore, this introduction of adaptation method allowed us to determine a reasonable P or t value for statistical analysis of functional imaging data.

Fig. 5 reveals that the threshold of T2* signal intensity can be set around 30 to separate IP-treated rats from normal ones. In other words, we may propose that if the T value in the hippocampus region is higher than 30, this subject may have predicting AD-like response. The threshold of T=30 may provide a quantitative evaluation for individuals with various pathological degenerative alterations. Moreover, all subjects in this study were scanned for at least 35 times. To further estimate the stability of the image sequence, the data were randomly divided into fore-and-aft two data sets. No obvious difference between them was indicated by Student's *t*-test, suggesting the reliability of image recording and analyzing. This suggests that, in contrast to high variability among individual subject, the intra-subject variability (L value ranges from 31.33 to 55.23) of BOLD fMRI is low, showing the stability of the imaging method. Despite the above advantages, there are also some potential questions in this methodology. For instance, the BOLD fMRI method do not directly detect electrical activity, but rely on the secondary and tertiary metabolic and hemodynamic events that accompany neuronal activity, which will cause nonlinear effects on the deduced results. The statistical analysis between control and IP-treated group, using one-tailed Student's *t*-test is also nonlinear with T2* signal intensity and add more uncertainty to the result. The neural system itself has high complexity with local specialization and global integration. In this paper, we performed an fMRI single subject statistic assess approach for experimental induced animal models base on linear regression analysis so that the biological diversity and artificial factors such as scan number, statistical model design, and signal-to-noise can be partially eliminated. However, further studies are needed in establishing a connection between behave change and T2* signal to obtain analogous sensitivity threshold.

Taken together, this study provided some extent information in supporting the potential application of fMRI in assessing AD-like pathology.

Acknowledgements

The authors are grateful to Mr. Yue FENG and Mr. Yunhuang YANG from Wuhan Institute of Physics and Mathematics, State Key Laboratory of Magnetic Resonance and Atomic and Molecular Physics, Chinese Academy of Sciences, for their performing the fMRI experiment.

References

1 Selkoe DJ. Alzheimer's disease is a synaptic failure. Science, 2002, 5594: 789–791
2 Gotz J, Chen F, van Dorpe J, Nitsch RM. Formation of neurofibrillary tangles in P301l tau transgenic mice induced by Abeta 42 fibrils. Science, 2001, 5534: 1491–1495
3 Kawabata S, Higgins GA, Gordon JW. Amyloid plaques, neurofibrillary tangles and neuronal loss in brains of transgenic mice overexpressing a C-terminal fragment of human amyloid precursor protein. Nature, 1991, 354(6353): 476–478
4 Larson EB, Shadlen MF, Wang L, McCormick WC, Bowen JD, Teri L, Kukull WA. Survival after initial diagnosis of Alzheimer disease. Ann Intern Med, 2004, 140(7): 501–509
5 Ferris SH, Yan B. Differential diagnosis and clinical assessment of patients with severe Alzheimer disease. Alzheimer Dis Assoc Disord, 2003, 17(Suppl3): S92–S95
6 Delacourte A, Sergeant N, Wattez A, Maurage CA, Lebert F, Pasquier F, David JP. Tau aggregation in the hippocampal formation: An ageing or a pathological process? Exp Gerontol, 2002, 37(10-11): 1291–1296
7 Jack CR Jr, Petersen RC, O'Brien PC, Tangalos EG. MR-based hippocampal volumetry in the diagnosis of Alzheimer's disease. Neurology, 1992, 42: 183–188
8 Xanthakos S, Krishnan KR, Kim DM, Charles HC. Magnetic resonance imaging of Alzheimer's disease. Prog Neuropsychopharmacol Biol Psychiatry, 1996, 20:597–626
9 Li SJ, Li Z, Wu G, Zhang MJ, Franczak M, Antuono PG. Alzheimer disease: Evaluation of a functional MR imaging index as a marker. Radiology, 2002, 225: 253–259
10 Jack CR Jr, Petersen RC, Xu YC, Waring SC, O'Brien PC, Tangalos EG, Smith GE *et al*. Medial temporal atrophy on MRI in normal aging and very mild Alzheimer's disease. Neurology. 1997, 49: 786–794
11 Small SA, Wu EX, Bartsch D, Perera GM, Lacefield CO, DeLaPaz R, Mayeux R *et al*. Imaging physiologic dysfunction Neurotechnique of individual hippocampal subregions in humans and genetically modified mice. Neuron, 2000, 28: 653–664
12 Wang XC, Hu ZH, Fang ZY, Feng Y, Yang YH, Wang Q, Tang XW *et al*. Correlation of Alzheimer-like tau abnormal hyperphosphorylation and fMRI

BOLD intensity. Current Alzheimer Research, 2004, 1(2): 143–145
13 Sun L, Liu SY, Zhou XW, Wang XC, Liu R, Wang Q, Wang JZ. Inhibition of protein phosphatase 2A- and protein phosphatase 1-induced tau hyperphosphorylation and impairment of spatial memory retention in rats. Neuroscience, 2003, 4: 1175–1182
14 Paxinos G, Watson C, Pennisi M, Topple A. Bregma, lambda and the interaural midpoint in stereotaxic surgery with rats of different sex, strain and weight. J Neurosci Methods, 1985, 13(2): 139–143
15 Liu SJ, Zhang AH, Li HL, Wang Q, Deng HM, Netzer WJ, Xu H *et al*. Overactivation of glycogen synthase kinase-3 by inhibition of phosphoinositol-3 kinase and protein kinase C leads to hyperphosphorylation of tau and impairment of spatial memory. J Neurochem, 2003, 87(6): 1333–1344
16 Friston KJ, Frith CD, Liddle PF, Dolan RJ, Lammertsma AA, Frackowiak RSJ. The relationship between global and local changes in PET scans. J Cereb Blood Flow Metab, 1990, 10: 458–466
17 Friston KJ, Holmes AP, Worsley KJ, Poline JP, Frith CD, Frackowiak RSJ. Statistical parametric maps in functional imaging: A general linear approach. Human Brain Mapping, 1995, 2: 189–210
18 Feany MB, Dickson DW. Neurodegenerative disorders with extensive tau pathology: A comparative study and review. Ann Neurol, 1996, 40(2): 139–148
19 Grundke-Iqbal I, Iqbal K, Quinlan M, Tung YC, Zaidi MS, Wisniewski HM. Microtubule-associated protein tau. A component of Alzheimer paired helical filaments. J Biol Chem, 1986, 261: 6084–6089
20 Hampel H, Goernitz A, Buerger K. Advances in the development of biomarkers for Alzheimer's disease: from CSF total tau and $A\beta_{1-42}$ proteins to phosphorylated tau protein. Brain Research Bulletin, 2003, 61(3): 243–253
21 Hu YY, SS He, Wang XC, Duan QH, Grundke-Iqbal I, Iqbal K, Wang JZ. Levels of nonphosphorylated and phosphorylated tau in CSF of Alzhemer disease: An ultrasensitive bienzyme-substrate-recycle ELISA. Am J Pathol, 2002, 160(4): 1269–1278
22 Mitchell A, Brindle N. CSF phosphorylated tau—does it constitute an accurate biological test for Alzheimer's disease? Int J Geriatr Psychiatry, 2003, 18(5): 407–411
23 Logothetis NK, Pauls J, Augath M, Trinath T, Oeltermann A. Neurophysiological investigation of the basis of the fMRI signal. Nature, 2001, 412: 150–157
24 Greicius MD, Strivatava G, Reiss AL, Menon V. Default-mode network activity distinguishes Alzheimer's disease from healthy aging: Evidence from functional MRI. Proc Natl Acad Sci USA, 2004, 101: 4637–4642

Edited by
Jia-Wei ZHOU